International Journal of Pharmaceutics 360 (2008) 83–90

Contents lists available at ScienceDirect

International Journal of Pharmaceutics

journal homepage: www.elsevier.com/locate/ijpharm

Influence of molecular organization and interactions on drug release for an injectable polymer-lipid blend

Justin Grant[a], Helen Lee[a], Patrick Lim Soo[a], Jaepyoung Cho[a], Micheline Piquette-Miller[a], Christine Allen[a,b,*]

[a] Department of Pharmaceutical Sciences, Leslie Dan Faculty of Pharmacy, University of Toronto, 144 College Street, Toronto, Ontario, Canada M5S 3M2
[b] Department of Chemistry, Faculty of Arts and Science, University of Toronto, 80 St. George Street, Toronto, Ontario, Canada M5S 3H6

ARTICLE INFO

Article history:
Received 28 January 2008
Received in revised form 30 March 2008
Accepted 12 April 2008
Available online 26 April 2008

Keywords:
Chitosan
Phospholipid
Paclitaxel
Injectable
Local drug delivery
Blend

ABSTRACT

An injectable blend composed of a water soluble chitosan (WSC) derivative, egg phosphatidylcholine (ePC), and fatty acid chlorides (FACl) was explored for localized delivery of anticancer agents. The composition–property relationships of the injectable WSC–FACl–ePC blend were determined by investigating the physico-chemical and performance properties of the blend as a function of the ratio of the components, as well as the acyl chain length of the FACl (C10–C16) employed. Thermal and rheological measurements revealed that the melting transitions and viscosities of the blends increased as a function of FACl acyl chain length. FTIR analysis demonstrated that the stability of the blends was attributed to the specific interactions among the molecules. In addition, confocal laser scanning microscopy revealed that the incorporation of C10–C16 FACl altered the molecular organization of ePC and WSC within the blends, which resulted in distinct physico-chemical properties. Specifically, the formation of micro-domains within the blends increased the stability, as well as delayed the release of paclitaxel from the formulation under physiologically relevant conditions. Overall, the interactions identified among the components, and the relationships established between the composition and properties of the blend can be used as a tool to develop advanced injectable drug delivery systems for pharmaceutical applications.

1. Introduction

Implantable and injectable depot systems have been widely explored for local and systemic delivery of drugs (Kalorama Information, 2007). In 2006, approximately 10 billion dollars of revenue was generated worldwide from drugs relying on formulation in implantable or injectable systems (Kalorama Information, 2007). Injectable formulations are particularly desirable due to their ease of administration and patient compliance. However, the design of injectable depot systems is challenging since numerous criteria must be considered including biocompatibility, biodegradation, stability and localization at the site of injection, rheological and thermal properties, as well as drug loading capacity and release profile.

Lupron Depot® is one of the first and most successful polymer-based injectable depot systems on the market that consists of poly(lactic-*co*-glycolic acid) (PLGA) microspheres (Sinha and Trehan, 2005). Several other injectable formulations that rely on PLGA microspheres have entered clinical trial development (Dunbar et al., 2006; Paquette, 2002). In addition to microsphere-based formulations, pastes and gels have also been explored as injectable depot systems (Almadrones, 2003; Hatefi and Amsden, 2002). For example, a Phase I study of a thermosensitive gel composed of an ABA triblock of PLGA and poly(ethylene glycol) (i.e. Oncogel®, Macromed Inc.) was recently reported for the localized delivery of the anticancer agent paclitaxel (PTX) in the treatment of solid tumours (Vukelja et al., 2007).

Local drug delivery offers several advantages over traditional systemic therapy by effectively delivering the pharmaceutical agent directly to the site of administration (Dhanikula and Panchagnula, 1999; Grant and Allen, 2006). In this way, local delivery can result in higher drug concentrations (20–1000-fold) at a targeted site, prolonged drug exposure, and reduced systemic toxicity (Agarwal and Kaye, 2003; Dhanikula and Panchagnula, 1999; Hatefi and Amsden, 2002; Ho et al., 2006; Langer, 1983; Markman, 1996). To this point, the injectable systems that have been explored are mostly formed from polyester materials (e.g. PLGA) which have been shown to induce a foreign body response that can result in the encapsulation of the device in a collagenous tissue (i.e. capsid formation) (Hickey et al., 2002). Therefore, there is a

* Corresponding author at: Leslie Dan Faculty of Pharmacy, University of Toronto, 144 College Street, Toronto, Ontario, Canada M5S 3M2. Tel.: +1 416 946 8594; fax: +1 416 978 8511.
E-mail address: cj.allen@utoronto.ca (C. Allen).

0378-5173/$ – see front matter © 2008 Elsevier B.V. All rights reserved.
doi:10.1016/j.ijpharm.2008.04.031

need to design new injectable formulations without polyesters in order to achieve biocompatibility at the site of administration, especially if long-term delivery is desired. In this connection, there has been an increased interest in the use of the natural polysaccharide chitosan for development of depot systems. A thermosensitive chitosan-glycerophosphate blend (BST-Gel®) developed by BioSyntech Inc. (Laval, Quebec, Canada) is currently in clinical trial for cartilage repair (Ruel-Gariepy et al., 2004). Previously, our group has reported the use of an implantable film composed of chitosan and egg phospatidylcholine (ePC) for the local delivery of PTX (Grant et al., 2005; Grant and Allen, 2006; Grant et al., 2007; Ho et al., 2005; Ho et al., 2006; Lim Soo et al., 2008; Vassileva et al., 2007). Due to the invasive nature of surgically implanting the film within the body, an injectable formulation with similar functional attributes, improved ease of administration and patient compliance was pursued.

In this paper, a blend of a water soluble chitosan (WSC) derivative, ePC, and fatty acid chloride (FACl) was examined as an injectable formulation for PTX. The acyl chain length of the FACl was varied and the stability, thermal and rheological properties of the injectable blends were measured. FTIR analysis identified the interactions among the components that are crucial in maintaining the structural integrity of the blends. The molecular organization of both the WSC and lipid components within the C10 to C16 blends was studied by confocal fluorescent microscopy. Lastly, the release of PTX from the blends was determined as a function of the acyl chain length of the FACl. Overall, changing the composition of the blend (i.e. varying the acyl chain length of the FACl and the relative ratios of each component) altered the molecular organization, and in turn affected the performance properties of the injectable formulation for drug delivery.

2. Materials and methods

2.1. Materials

Chitosan (92.5% purity) was purchased from Marinard Biotech Inc. (Rivière-au-Renard, QC, Canada). The chitosan contained 8% β-(1-4)-2-acetamido-D-glucose (i.e. chitin) and 92% β-(1-4)-2-amino-D-glucose units (i.e. chitosan). The fluorescent probes, Alexa Fluor® 633 and 1,2-dipalmitoyl-sn-glycero-3-phosphoethanolamine-*N*-(7-nitro-2-1,3-benzoxadiazol-4-yl) (NBD-DPPE) were purchased from Molecular Probes Inc. (Eugene, OR) and Avanti Polar Lipids Inc. (Alabaster, AL), respectively. Unlabelled PTX (>99%) and ^{14}C-PTX were purchased from Hande Tech Development Co. (Houston, TX) and Moravek (Brea, CA), respectively. Egg phosphatidylcholine (ePC), glycidyltrimethylammonium chloride (GTMAC), acetone, ethanol, methanol, acetic acid (AcOH), fatty acid chlorides (i.e. decanoyl chloride (C10), lauroyl chloride (C12), myristoyl chloride (C14) and palmitoyl chloride (C16)) and all other chemicals were purchased from Sigma–Aldrich Chemical Co. (Oakville, ON, Canada). All chemicals were reagent grade and used without further purification.

2.2. Blend preparation

The WSC derivative, composed of GTMAC and chitosan in a ratio of 3:1 (mol/mol), was synthesized using an established method that is described in detail elsewhere (Cho et al., 2006; Seong et al., 2000). Excess GTMAC was removed using methanol followed by precipitation of the polymer in acetone. This procedure was repeated in triplicate and the WSC was then dried in a vacuum oven prior to use. For preparation of the WSC–FA–ePC blend, WSC was first dissolved in distilled water to prepare a 4.2% (w/v) WSC solution. EPC was solubilized in FACl, which varied in terms of acyl chain length (i.e. C6 to C16) and then added to the WSC solutions at specific weight ratios. Lastly, the WSC–FACl–ePC blend was vortexed for 2 min and stored at room temperature. For preparation of the drug loaded blends, 5 μCi of the ^{14}C-PTX in ethyl acetate was added to 10 mg of PTX and dried under nitrogen to form a thin film of drug. A FACl-lipid solution containing C12, C14 or C16 FACl and ePC was used to resuspend the PTX film prior to mixing with WSC to achieve a WSC–FACl–ePC–PTX (1:4:1:0.25 (w/w/w/w)) blend.

2.3. Characterization of stability and pH profile

The stability of the blends varying in FACl chain length in buffer containing lysozyme was assessed by turbidity measurements. Approximately 300 μL of the WSC–FACl–ePC blend was injected into a vial containing 0.01 M PBS (pH 7.4) and 0.2% lysozyme as chitosan is known to degrade in the presence of lysozyme (Grant et al., 2005; Hirano et al., 1989). At specific time points, an aliquot of the solution was analyzed using UV spectroscopy at $\lambda = 700$ nm (Cary 50 UV–vis spectrophotometer, Varian Inc., Palo Alto, CA). The aliquot was then placed back into the vial containing the blend for subsequent analysis. The stability of the WSC–FACl–ePC blends was also visually inspected during preparation and following injection into 5 mL of 0.01 M PBS (pH 7.4) over a 72 h period at 37 °C. At specific time points, the PBS solution was removed from each vial and stirred prior to measurement of pH.

2.4. Thermal analysis

A differential scanning calorimeter (DSC) Q100 (TA Instruments, New Castle, DE) was used to determine the melting transitions of the WSC–FACl–ePC blends. Samples of 5–7 mg were placed in hermetic pans and their transition temperatures were analyzed between −20 °C and 80 °C at a temperature ramp speed of 5 °C/min under nitrogen purge. TA universal analysis software was used to analyze the second heating cycle of all samples.

2.5. FTIR analysis

The FTIR spectra of the WSC–FACl–ePC blends and their individual components were obtained using a universal ATR Spectrum-one spectrophotometer (Perkin-Elmer, Wellesley, MA). The samples were prepared as thin films and a background spectrum of air was subtracted from the sample spectra using Perkin-Elmer's Spectrum software. All spectra were an average of 16 scans at a resolution of 2 cm^{-1} and repeated in triplicate.

2.6. Morphology

Images of the 1:4:1 (w/w/w) WSC–FACl–ePC blends containing C10, C12, C14 or C16 FACl were obtained by an inverted two-photon confocal laser scanning fluorescence microscope (Zeiss LSM 510 META NLO, Germany). Regions of WSC and lipid within the blend were identified using fluorescently labeled WSC and DPPE. The amine reactive fluorescent probe, succinimidyl ester of Alexa Fluor 633 ($\lambda_{ex} = 632$, $\lambda_{em} = 647$), was used to label WSC. The conjugation of Alexa Fluor 633 to the amine groups of WSC was performed according to the manufacturer's protocol and confirmed by FTIR analysis (data not shown) (Molecular Probes, Eugene, OR). Using UV measurements, it was estimated that 0.1% of monomer units on the polymer chain were modified by the chromophore (data not shown). To prepare the fluorescently labeled WSC–FACl–ePC blends, 1 mol% of the fluorescent phospholipid NBD-DPPE ($\lambda_{ex} = 460$ nm, $\lambda_{em} = 534$ nm) was dissolved in ethanol and dried to a film using nitrogen (Grant et al., 2007). Pure ePC

was dissolved in FACl and mixed with the fluorescent lipid film. The FACl–ePC solution was mixed with WSC containing 1% (w/w) of the Alexa Fluor 633 conjugated WSC to prepare a 1:4:1 blend which was cast onto a glass slide. Cover slips were placed on the solution and the formulation was dried in the dark overnight. Colocalization analyses including generation of colocalization maps, colocalization coefficients, measurement of object areas, and mean gray values were obtained by Image-Pro Analyzer V6.0 (Media Cybernetics Inc, Bethesda, MD, USA).

2.7. Rheological measurements

The rheological properties of WSC–FACl–ePC blends were characterized by a stress-controlled rheometer with a 2 cm cone and 4° angle plate geometry at room temperature (AR-2000, TA Instruments). The rheometer was calibrated and rotational mapping was performed according to instrument specifications. The viscosity was measured using a continuous ramping flow mode while increasing the shear stress from 1 to 500 Pa. The blend formulations were stored for 24 h prior to mechanical testing. A 200 μL injection of each sample was placed on the rheometer plate for mechanical testing.

2.8. Drug release

Approximately 300 μL of the WSC–FACl–ePC blend, which contained a mixture of ^{14}C-PTX (0.14 μCi) and cold PTX (10 mg) (i.e. drug to material ratio of 1:24 (w/w)) was injected into a vial containing 5 mL of 0.01 M PBS (pH 7.4) with 0.2% lysozyme. The samples were incubated at 37 °C and at specific time points, the vials were agitated and 2.5 mL of solution was removed from each vial and replaced with 2.5 mL of fresh PBS/lysozyme solution. A 4 mL aliquot of Ready Safe liquid scintillation cocktail (Beckman Coulter Inc., Fullerton, CA) was added to each sample, vortexed and then analyzed by scintillation counting (Beckman LS 5000 TD, Beckman Instruments Inc., Fullerton, CA).

3. Results and discussion

3.1. Preparation and optimization of blend composition

The injectable blend was prepared from three components: a water soluble chitosan derivative, fatty acid chloride and egg phosphatidylcholine. The WSC was prepared by conjugation of GTMAC to the amine groups of chitosan in a 3:1 molar ratio as confirmed by FTIR (data not shown). As determined previously, 56% of the chitosan chain contained GTMAC (i.e. degree of substitution) at this molar ratio (Cho et al., 2006). The hydrophilic component of the blend consisted of WSC, which dissolved in distilled water at a concentration of 42 mg/ml. Employing the WSC avoids the use of an acidic solution, which would otherwise be required to dissolve the biopolymer chitosan (pK_a = 6.5 for 400 kDa chitosan). For preparation of an injectable blend that remains stable in an aqueous environment, a balance between the hydrophilic and hydrophobic components must be achieved. Thus, FACl and ePC were employed within the blend to increase the overall hydrophobicity. EPC is a mixture of phosphatidycholine lipids that vary in acyl chain length (i.e. C16:0 (34%), C18:1 (32%), C18:2 (18%), C18:0 (11%), C20:4 (3%) and C16:1 (2%)). It has been established that ePC interacts with the amine groups of WSC; however, the degree of interaction and/or hydrophobicity was found to be insufficient to produce a stable injectable blend. In contrast to the solid-based fatty acids (i.e. RCOOH), FACls are liquids that have a higher reactivity in aqueous media. Thus, FACl varying in acyl chain length (i.e. C10–C16) was incorporated within the blend and was found to mix well with both WSC and ePC.

FACls are known to undergo hydrolysis in the presence of water as the carbon–chloride bond of the FACl is easily cleaved to produce a fatty acid and hydrogen chloride (Sonntag, 1953). Bauer and Curet investigated the rate of hydrolysis for FACl in water at 25 °C and found that longer chain length FACl (i.e. C16 and C18) had a more rapid rate of hydrolysis than the FACls with shorter chain lengths (i.e. C8–C14) (Bauer and Curet, 1947). Interestingly, during the first several hours of incubation in water, C12 FACl was the most resistant to hydrolysis. The mole percentage of C10–C16 unhydrolyzed FACl reached a plateau that ranged from approximately 3–45% within 24 h of the reaction (Bauer and Curet, 1947). Thus, the series of experiments in this study were performed at least 24 h following preparation of the blends to allow for the maximum degree of hydrolysis of FACl to occur.

The stability of the WSC–FACl–ePC blends was assessed by visually observing the formulations following injection into 0.01 M PBS (pH 7.4) at 37 °C over a 72-h period. The stability of the blends was found to be dependent on both the acyl chain length of the FACl employed and the ratio of the three components. For example, the blend containing C12 FACl disintegrated in buffer solution upon injection when the concentration of WSC was below 17 wt% or 42 mg/mL. A minimal concentration of the WSC is likely required due to the need for stabilizing interactions between the amine groups, of the glucosamine residues on the biopolymer, and various functional groups on other components of the blend. The blend was also unstable at high concentrations of WSC (i.e. >23 wt% or 57 mg/ml) as the components were more difficult to mix due to the viscosity of the WSC. It was also found that at least 66 wt% FACl and 10 wt% ePC were required to stabilize the formulation in buffer over the 72-hour incubation period. From these results, a 1:4:1 (w/w/w) (i.e. 17:66:17 wt%) WSC–FACl–ePC blend ratio was used to investigate the effect of FACl chain length.

The stability of the WSC–FACl–ePC (1:4:1) blends as a function of acyl chain length (C10–C16 FACl) was further evaluated by turbidity measurements in 0.2% lysozyme and 0.01 M PBS at 37 °C over a two-month incubation period (Supplemental Fig. S1). The semi-solid C10 FACl blend disintegrated upon injection into the lysozyme solution. However, the formulations that contained C12 to C16 FACl were stable as indicated by low absorbance values after 1 h. The blend containing the C12 FACl was considered most stable as the absorbance values remained the lowest over the two-month incubation period. Similarly, Rinaudo et al. showed that a C12 alkylated chitosan was the optimal chain length that formed a gel with hydrophobic domains and network junctions (Rinaudo et al., 2005). In addition, a study revealed that blends prepared from chitosan and C12 fatty acid had the lowest water permeability (Wong et al., 1992).

3.2. Evaluation of material interactions and miscibility

3.2.1. FTIR analysis

In order to determine the interactions that stabilize the 1:4:1 (w/w/w) WSC–FACl–ePC blends, FTIR spectra of the blends and their individual components were analyzed (Fig. 1). The WSC spectrum contained a large broad peak at 3300 cm^{-1} which represented the O—H groups of the polymer and water molecules (labeled as (a) in Fig. 1). In addition, N—H bending of the primary amine groups of chitosan and C=O stretching of the secondary amide of chitin were observed at 1564 and 1640 cm^{-1}, respectively. In agreement with the literature, an interaction between WSC and ePC was observed by a shift in the peak representing the primary amine groups of WSC from 1564 to 1575 cm^{-1} with the addition of lipid (Cho et al., 2006).

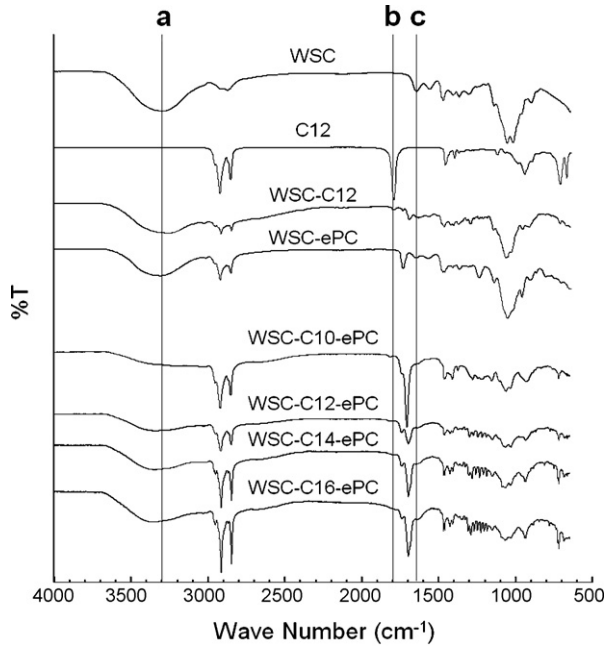

Fig. 1. FTIR spectra of water soluble chitosan (WSC), lauroyl chloride (C12), WSC–C12 FACl blend (1:4, w/w), WSC–ePC blend (1:1, w/w) and 1:4:1 (w/w/w) WSC–FACl–ePC blends varying in FACl acyl chain length from C10 to C16.

For the spectra of the C10 to C16 FACl alone, the peak positions for each of the functional groups were nearly identical (C12 FACl is shown in Fig. 1). The spectra contained sharp peaks at 1800 cm^{-1} (labeled as line (b) in Fig. 1) and 720 cm^{-1} which represent the acid chloride group (COCl) and C—Cl bond, respectively (De Lorenzi et al., 1999; Fang et al., 2004; Foucault et al., 2001; Williams and Fleming, 1987). For the WSC–FACl blends, a small peak was observed at 1800 cm^{-1} signifying that the FACl was not completely hydrolyzed following the 24-h period (Fig. 1). The primary amine group of WSC may also interact with the unhydrolyzed acid chloride group of FACl as shown in the reaction scheme below (Sonntag, 1953):

$$RCOCl + 2R'NH_2 \rightarrow RCONHR' + R'NH_3Cl \quad (1)$$

Acylation of the amine groups on the glucosamine residues of the WSC by FACl produces amide groups (i.e. RCONHR′) and HCl, which can then further react with free amine groups to produce a salt (i.e. $R'NH_3Cl$). A broadening of the 1640 cm^{-1} peak (labeled as line (c) in Fig. 1) and 1564 cm^{-1} peak were observed for the 1:4 (w/w) WSC–FACl blends, which may be due to the formation of the amide and amine salt (Eq. (1)) (Fang et al., 2004). In addition, a new peak appeared at 1700 cm^{-1} which represents the carboxylic acid group that formed during the hydrolysis reaction of FACl (Fang et al., 2004; Williams and Fleming, 1987). A significant reduction in the area (i.e. approximately 80%) of the C—Cl peak at 720 cm^{-1} provides further evidence that the acid chloride group of FACl was hydrolyzed in the WSC–FACl blends. A weak transmittance peak at 1740 cm^{-1} was observed which may represent the esterification of FACl or *O*-acylation of WSC (Fang et al., 2004; Hirano et al., 1976). Although substitution reactions can occur on both amine and hydroxyl groups of WSC, amine groups are generally more reactive than hydroxyl groups (Fujii et al., 1980; Roberts, 1992). However, the conditions are not favorable for *N*-acetylation of WSC due to the high reactivity of FACls in the aqueous environment, as well as the steric effects present between the WSC molecules (Roberts, 1992). Using a method first described by Moore and Roberts, the degree of *N*-acetylation was estimated from the ratio of absorbance at the amide group at 1640 cm^{-1} and the hydroxyl group at 3300 cm^{-1} (Le Tien et al., 2003; Moore and Roberts, 1980). For the C16–C10 FACl and WSC blends, the degree of substitution on the WSC backbone ranged from 2 to 10%, respectively.

For the 1:4:1 (w/w/w) WSC–FACl–ePC blends, the area of the peak representing the O—H groups of WSC at 3300 cm^{-1} was smaller for WSC–FACl–ePC than WSC–FACl and WSC–ePC blends, indicating an increase in hydrophobicity for the ternary blends (labeled as line (a) in Fig. 1). Interestingly, the O—H peak area increased as the FACl acyl chain length increased within the WSC–FACl–ePC blends. Although the amine groups of WSC (i.e. peak at 1564 cm^{-1}) were difficult to detect, a shift in the peak representing the amide groups of WSC was observed from 1640 to 1628 cm^{-1} for all the blends (labeled as line (c) in Fig. 1). Thus, ePC may provide a more favorable environment for WSC to interact with FACl. The absence of a defined peak at 1800 cm^{-1} in all the WSC–FACl–ePC blends indicated that the acid chloride group of FACl was hydrolyzed and/or interacted with the amine groups of WSC or groups within ePC. Further evidence of these reactions within the C10–C16 FACl blends were observed by a significant decrease in the pH of 0.01 M PBS solution from 7.4 to approximately 2.0 within the first hour of incubation (Supplemental Fig. S2). The decrease in pH is attributed to the formation of acid byproducts of FACl during the reaction with water and/or WSC.

FTIR analysis also revealed that the carboxylic acid band at 1700 cm^{-1} in the WSC–FACl blends became even more prominent with the addition of ePC and was found to shift to 1708 cm^{-1} for only the C10 blend. Furthermore, the peak area decreased by approximately 50% for the C12 WSC–FACl–ePC blend. Thus, the stability found for the WSC–FACl–ePC blend containing C12 FACl may be related to interactions involving the carboxylic acid groups of the hydrolyzed FACl. Also, a large number of small peaks were observed between 1200 and 1400 cm^{-1} which may be attributed to CO stretching of the hydrolyzed FACl as well as the choline headgroup of the lipid (Williams and Fleming, 1987). Interestingly, the number of peaks in this region increased with increasing FACl chain length. Overall, it is postulated that the amine and hydroxyl groups of WSC, the carboxylic acid groups and acyl chains of the hydrolyzed FACls and the phosphatidylcholine headgroup of ePC are involved in stabilizing the blend formulation.

3.2.2. Thermal analysis

The thermal behavior of WSC, ePC and each of the FACl revealed a single melting transition (T_m) for each component as shown in Table 1. For 4.2% (w/v) WSC solution, an endothermic peak was present at approximately 2.8 °C, which did not interfere with the T_m of ePC and FACl. Specifically, a single broad T_m for ePC was observed at approximately 26 °C due to the heterogeneity of the lipid (Grant et al., 2007). The T_m of FACl (i.e. C10 to C16) increased with increas-

Table 1
The chain length (L_c), melting temperature (T_m) and molecular weight (MW) for water soluble chitosan (WSC), egg phosphatidylcholine (ePC), fatty acid chlorides (FACl) and fatty acids

Sample	L_c	T_m (°C)	MW (g/mol)
WSC (42 mg/mL)	–	2.8	400,000
ePC	C16–C20	26.0	760.1
Decanoyl acid chloride	C10	−31.4	190.7
Lauroyl chloride	C12	−17.6	218.8
Myristoyl chloride	C14	0.2	246.8
Palmitoyl chloride	C16	12.1	274.9
Decanoic acid[a]	C10	27–32	172.3
Lauric acid[a]	C12	44–46	200.3
Myristic acid[a]	C14	52–54	228.4
Palmitic acid[a]	C16	61–62.5	256.4

[a] Values obtained from the manufacturer, Sigma–Aldrich.

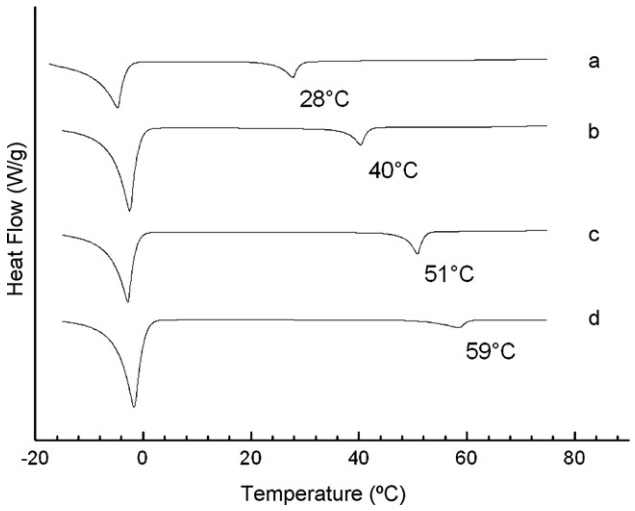

Fig. 2. DSC thermograms of (1:4:1, w/w/w) WSC–FACl–ePC blends containing C10 FACl (a), C12 FACl (b), C14 FACl (c) and C16 FACl (d). *Note*: Peaks are in the endothermic direction.

ing acyl chain length and ranged from approximately −31 to 12 °C. These values are significantly lower than the T_m for fatty acids of the same chain length (Table 1).

In order to assess the miscibility of the (1:4:1, w/w/w) WSC–FACl–ePC blends, the T_m for binary mixtures of (1:4, w/w) WSC–FACl were first evaluated (Supplemental Fig. S3). For the WSC–FACl blends, two peaks were observed that corresponded to the FACl and WSC components. The melting peak for WSC occurred between −1.5 and −3.5 °C, while the T_m for the C10 to C16 FACl ranged from 18 °C to 59 °C, respectively. The increase in T_m for FACl is mostly attributed to the hydrolysis reaction of FACl in the presence of water as discussed above (Bauer and Curet, 1947). The C12 WSC blend had a smaller peak area for WSC at −2.7 °C which supports the interactions observed between WSC and C12 FACl by FTIR analysis.

The T_m for the WSC–FACl–ePC (1:4:1) blends with increasing FACl chain length is shown in Fig. 2. Interestingly, only two peaks were observed from the thermograms; one at a low temperature (i.e. −4.7 to −1.5 °C) and the other T_m at a higher temperature (i.e. 28–59 °C). Thus, a degree of miscibility was observed between the FACl and ePC as only a single T_m was found for these components in the temperature range investigated. Furthermore, the T_m was found to increase in temperature from 28 °C to 59 °C with increasing FACl chain length. Comparing the difference in T_m (ΔT) for the WSC–FACl blends with and without ePC (e.g. WSC–C12 FACl vs. WSC–C12 FACl–ePC), the ΔT increased linearly as the FACl chain length decreased. Specifically, ΔT was 10 °C for C10, 7 °C for C12, 5 °C for C14, and no change in ΔT was observed for the C16 blends. Thus, ePC may have a lower miscibility with FACl of longer acyl chain lengths, which may explain the decreased stability observed for the C16 FACl blend.

3.2.3. Morphology

Confocal laser scanning microscopy was used to identify the regions containing WSC and lipid, as well as to determine the effect of increasing FACl acyl chain length on the morphology of the (1:4:1, w/w/w) WSC–FACl–ePC blends (Fig. 3). The red regions shown in Fig. 3b, f, j, and n represent the WSC component; while the green fluorescent regions in Fig. 3a, e, i, and m correspond to the lipid component. Fig. 3c, g, k, o were overlays of the ePC and WSC components of the C10–C16 WSC–FACl–ePC blends, respectively. The yellow regions in the overlay images indicate areas of colocalization for WSC and ePC. The black regions may correspond to the unlabelled FACl or the uneven surface of the film.

The presence of the domains was critical in stabilizing the blends following injection into the buffer solution (Supplemental Fig. S1). A previous study showed that the formation of large sized lipid domains within chitosan-ePC films contributed to enhanced stability (Grant et al., 2007). In contrast, for the C10 WSC–FACl–ePC blend, the absence of domains and the fact that the FTIR spectra peak representing the carboxylic acid group of the hydrolyzed FACl appeared at a higher wave number than the other blends support the instability observed for the C10 blend (Figs. 1 and 3).

The interaction between ePC and WSC as a function of FACl acyl chain length was further examined by the degree of ePC–WSC colocalization. The specific intermolecular interactions that were detected by FTIR analyses are more likely to occur at the colocalized regions due to the close proximity of the functional groups in each component. As shown in Fig. 3c, g, k, o and Table 2, ePC and WSC were found to colocalize in larger domains (i.e. yellow regions) in the blends containing C12 and C14 (i.e. mean object areas of 8.5 and 6.3 μm^2) when compared to the C16 blend (i.e. mean object area of 3.5 μm^2). In order to quantify the extent to which ePC–WSC colocalized, colocalization maps were generated (Fig. 3d, h, l, and p). Each yellow pixel (ePC–WSC colocalization) detected in Fig. 3c, g, k, and o is represented by a bright pixel (white) in the corresponding colocalization maps. The mean gray values within the colocalization maps (i.e. amount of bright pixels relative to the background) were 30, 25, and 15 for the WSC–FACl–ePC blends containing C12, C14, and C16 FACl, respectively (Table 2). In agreement with the stability and FTIR results, the degree of ePC/WSC interaction was highest for the C12 FACl blend. Similar results were also obtained from the colocalization coefficients M1 and M2, which represent the contribution of the lipid (green fluorescent signal) and WSC (red fluorescent signal) to the colocalized areas, respectively. As indicated in Table 2, approximately 42% of ePC and 39% of WSC colocalized within the C12 WSC–FACl–ePC blend in comparison to 21% of ePC and 26% of WSC in the C16 blend. In addition to the physical properties of the blend (i.e. thermal, morphology), the FACl chain length was also found to affect the performance properties of the WSC–FACl–ePC blends.

3.3. Evaluation of performance properties

3.3.1. Rheological analysis

The rheological properties of injectable drug delivery systems are important as a low viscosity blend may not exhibit a sustained drug release profile and a high viscosity blend may be difficult to administer (Hatefi and Amsden, 2002; Packhaeuser et al., 2004). In order to determine the optimal rheological proper-

Table 2
Colocalization analysis of the WSC and ePC regions within the 1:4:1 (w/w/w) WSC–FACl–ePC blends, with increasing FACl acyl chain length, from the confocal images (Fig. 3)

Acyl chain length	Mean object areas[a] (μm^2)	M1 (ePC)[b]	M2 (WSC)[b]	Mean gray value[c]
C10	–	38	40	50
C12	8.5	42	39	30
C14	6.3	33	32	25
C16	3.5	21	26	15

[a] Mean object areas represent the average area of the WSC–ePC colocalized domains in the colocalization maps (i.e. Fig. 3h, l, and p).

[b] M1 and M2 represent the percentage of lipid (green) and WSC (red) fluorescence signals in the colocalized area relative to the total lipid and WSC fluorescence signals, respectively.

[c] Mean gray values represent the amount of bright pixels detected in the WSC–ePC colocalization maps (i.e. Fig. 3d, h, l, and p).

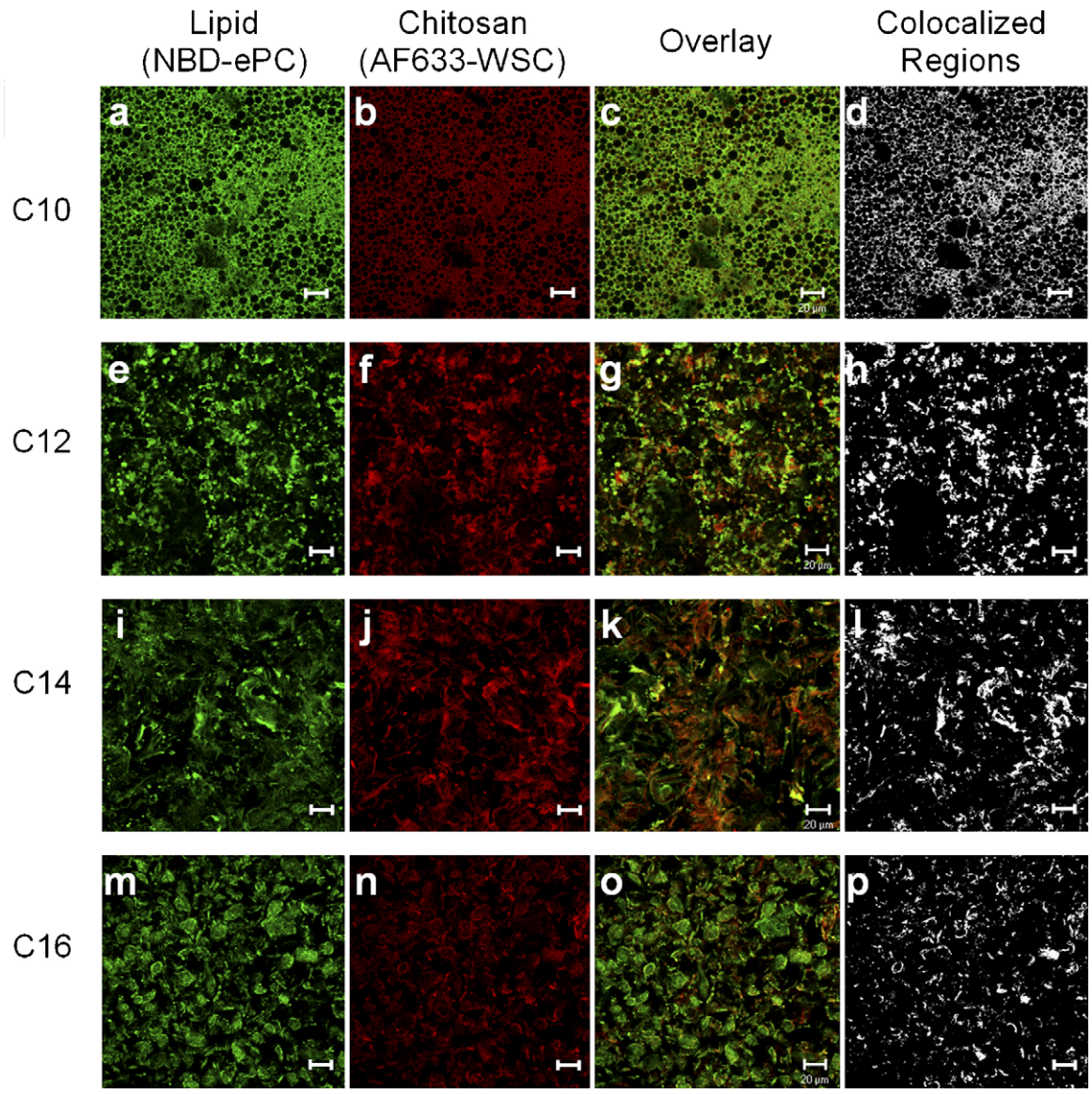

Fig. 3. Scanning confocal fluorescence microscopy images of the 1:4:1 (w/w/w) WSC–FACl–ePC blends containing C10 FACl (a–d), C12 FACl (e–h), C14 FACl (i–l) and C16 FACl (m–p) where lipid regions are in green (a, e, i, m), WSC is imaged in red (b, f, j, n) and the overlay of the WSC and FACl–ePC regions is in the third column (c, g, k, o). The regions where the lipid and the WSC colocalized are shown in the images in the forth column (d, h, l, p). The scale bar in each image represents 20 μm. (For interpretation of the references to color in this figure legend, the reader is referred to the web version of the article.)

ties of the injectable blend, the viscosities of the 1:4:1 (w/w/w) WSC–FACl–ePC blends were measured as a function of the FACl acyl chain length (i.e. C12–C16) using steady shear tests (Fig. 4). The WSC–FACl–ePC blend containing C10 FACl was not evaluated as this blend was found to be unstable in aqueous media and could not be employed for use as a long-term drug release system. As shown in Fig. 4, an increase in the FACl chain length in the WSC–FACl–ePC blend resulted in an increase in the viscosity and yield stress values. For example, at low shear stress (i.e. at 10^0 Pa), the blends containing the C14 and C16 FACl had a viscosity of approximately 1×10^5 Pa s, whereas the C12 FACl blend was approximately 1×10^3 Pa s. As the shear stress increased, an earlier non-Newtonian behavior was observed for the C12 FACl blend in comparison to the C14 and C16 FACl blends. Thus, the C12 FACl blend will require less force to flow through the needle of a syringe during injection. From the literature, most injectable systems use a 22 gauge needle size, otherwise special equipment such as hydraulic syringes are employed for more viscous solutions (Packhaeuser et al., 2004). From our results, only the WSC–FACl–ePC (1:4:1) blend containing C12 FACl was injectable via a 22 gauge needle. Thus, the optimal formulation ratio to produce a stable injectable blend was WSC–FACl–ePC (1:4:1) containing the C12 FACl.

3.3.2. Drug release

The influence of the FACl acyl chain length on the release of ^{14}C-PTX from the WSC–FACl–ePC (1:4:1, w/w/w) blends prepared from C12 to C16 FACl is shown in Fig. 5. An initial release of 19–28% of the total PTX loaded within the WSC–FACl–ePC blends was observed during the first 24 h of analysis. A complete release (i.e. 100%) of PTX was observed for the C16 FACl and C12 FACl blends following one week and three weeks, respectively. In contrast, the PTX release from the C14 FACl blend, reached 70% after 30 days, and continued at a sustained release rate of 0.2%/day for three months. Similarly, Guse et al. observed a slower release for pyranine from fatty acid glyceroltrimyristate (C14) when compared to glyceroltrilaurate (C12) and glycerolpalmitate (C16) (Guse et al.,

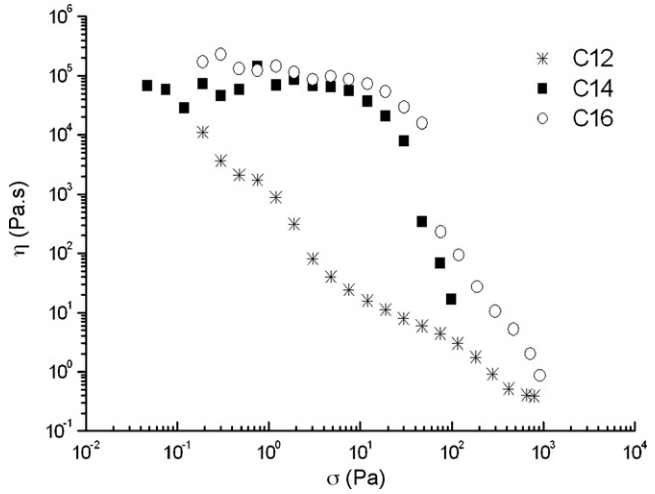

Fig. 4. The viscosity (η) as a function of shear stress (σ) for 1:4:1 (w/w/w) WSC–FACl–ePC blends that vary in FACl acyl chain length from C12 to C16.

2006). Vogelhuber et al. found that the release of pyranine from triglycerides matrices was strongly affected by the fatty acid chain length (Vogelhuber et al., 2003). In addition, Domb's group demonstrated that release of methotrexate from nonlinear fatty acid terminated polyanhydrides was dependent on the length of the fatty acid side chain (i.e. the longer the side chain, the slower the drug release) (Teomim and Domb, 2001).

In this study, the C14 FACl blend exhibited the slowest drug release rate which may be attributed to the larger hydrophobic lipid domains (Fig. 3i) within the blend when compared to the C12 and C16 FACl formulations (Fig. 3e and m). The larger hydrophobic domains within the blend result in a longer diffusion length for the drug. PTX is known to partition in hydrophobic phases due to its low aqueous solubility (Sparreboom et al., 1996). In addition, the rheological properties of the blends may also explain the slower drug release rate of PTX from the C14 blend when compared to the C12 blend. As shown in Fig. 4, the rheological properties for the 1:4:1 WSC–FACl–ePC blends were increased by approximately two orders of magnitude when a longer FACl acyl chain length was employed (i.e. $\eta \sim 10^3$ Pa s and $\eta \sim 10^5$ Pa s for C12 and C14, respectively). In general, the viscosity increases when there are more interactions between macromolecules such as entanglement, physical interactions (i.e. van der Waals, hydrophobic and hydrogen bonding) and cross-linking. These interactions can be used to trap the drug and reduce the rate of drug release. Interestingly, the C16 FACl blend was found to have the fastest drug release rate even though it has similar rheological properties to the C14 FACl blend. The rapid drug release profile observed for the C16 FACl blend may be attributed to the instability of the formulation as it was shown to degrade to a greater extent than the C12 and the C14 FACl blend (Supplemental Fig. S1). Overall, the drug release from the WSC–FACl–ePC blends can be controlled by modifying the chain length of the FACl component employed within the ternary blend.

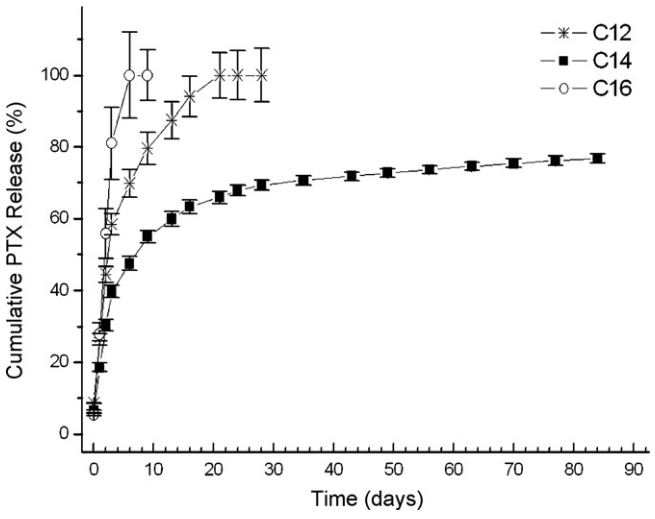

Fig. 5. The percent cumulative release of paclitaxel from the 1:4:1 (w/w/w) WSC–FACl–ePC blends varying in FACl acyl chain length from C12 to C16 as a function of time. Error bars are expressed as standard error ($n = 3$).

4. Conclusions

The combination of a WSC derivative, the lipid ePC, and FACl formed an injectable blend for localized delivery of the anticancer agent PTX. The ratio of the three components and the acyl chain length of the FACl employed were found to have a significant impact on the molecular organization and hence, the properties of the blend. From the established composition–property relationships, the ratio of 1:4:1 (w/w/w) WSC–FACl–ePC containing the C12 FACl was the most stable blend in aqueous media at physiological temperature, provided a sustained release of PTX over a three-week period, and was injectable via a 22 gauge needle. However, there are concerns regarding the toxicity of the formulation and the stability of some drugs due to the low pH that results following hydrolysis of FACl. Current efforts are focused on the replacement of FACl with non-hydrolyzable fatty acid derivatives.

Acknowledgements

The authors are grateful to NSERC for an operating grant to Prof. C. Allen, a PGS scholarship to J. Grant and a CIHR RX&D fellowship to Dr. P. Lim Soo. In addition, the authors are thankful to OCRN and CCS for research funding.

Appendix A. Supplementary data

Supplementary data associated with this article can be found, in the online version, at doi:10.1016/j.ijpharm.2008.04.031.

References

Agarwal, R., Kaye, S.B., 2003. Ovarian cancer: strategies for overcoming resistance to chemotherapy. Nat. Rev. Cancer 3, 502–516.
Almadrones, L.A., 2003. Treatment advances in ovarian cancer. Cancer Nurs. 26, 16S–20S.
Bauer, S.T., Curet, M.C., 1947. The hydrolysis of fatty acid chlorides. J. Am. Oil. Chem. Soc. 24, 36–39.
Cho, J., Grant, J., Piquette-Miller, M., Allen, C., 2006. Synthesis and physicochemical and dynamic mechanical properties of a water-soluble chitosan derivative as a biomaterial. Biomacromolecules 7, 2845–2855.
De Lorenzi, A., Giorgianni, S., Bini, R., 1999. High-resolution FTIR spectroscopy of the C-Cl stretching mode of vinyl chloride. Mol. Phys. 96, 101–108.
Dhanikula, A.B., Panchagnula, R., 1999. Localized paclitaxel delivery. Int. J. Pharm. 183, 85–100.
Dunbar, J.L., Turncliff, R.Z., Dong, Q., Silverman, B.L., Ehrich, E.W., Lasseter, K.C., 2006. Single- and multiple-dose pharmacokinetics of long-acting injectable naltrexone. Alcohol. Clin. Exp. Res. 30, 480–490.
Fang, J.M., Fowler, P.A., Sayers, C., Williams, P.A., 2004. The chemical modification of a range of starches under aqueous reaction conditions. Carbohyd. Polym. 55, 283–289.
Foucault, F., Esnouf, S., Le Moel, A., 2001. Irradiation/temperature synergy effects on degradation and ageing of chlorosulphonated polyethylene. Nucl. Instrum. Meth. B 185, 311–317.
Fujii, S., Kumagai, H., Noda, M., 1980. Preparation of poly(acyl)chitosans. Carbohyd. Res. 83, 389–393.
Grant, J., Allen, C., 2006. Chitosan as a biomaterial for preparation of depot-based delivery systems. In: Marchessault, R.H., Ravenelle, F., Zhu, X.X. (Eds.), Polysac-

charides for Drug Delivery and Pharmaceutical Applications. Oxford University Press Inc., Montreal, pp. 201–225.
Grant, J., Blicker, M., Piquette-Miller, M., Allen, C., 2005. Hybrid films from blends of chitosan and egg phosphatidylcholine for localized delivery of paclitaxel. J. Pharm. Sci. 94, 1512–1527.
Grant, J., Tomba, J.P., Lee, H., Allen, C., 2007. Relationship between composition and properties for stable chitosan films containing lipid microdomains. J. Appl. Polym. Sci. 103, 3453–3460.
Guse, C., Koennings, S., Blunk, T., Siepmann, J., Goepferich, A., 2006. Programmable implants—from pulsatile to controlled release. Int. J. Pharm. 314, 161–169.
Hatefi, A., Amsden, B., 2002. Biodegradable injectable in situ forming drug delivery systems. J. Control. Rel. 80, 9–28.
Hickey, T., Kreutzer, D., Burgess, D.J., Moussy, F., 2002. In vivo evaluation of a dexamethasone/PLGA microsphere system designed to suppress the inflammatory tissue response to implantable medical devices. J. Biomed. Mater. Res. 61, 180–187.
Hirano, S., Ohe, Y., Ono, H., 1976. Selective N-acylation of chitosan. Carbohyd. Res. 47, 315–320.
Hirano, S., Tsuchida, H., Nagao, N., 1989. N-acetylation in chitosan and the rate of its enzymic hydrolysis. Biomaterials 10, 574–576.
Ho, E., Vassileva, V., Lim-Soo, P., Allen, C., Piquette-Miller, M., 2006. Impact of localized, sustained delivery of paclitaxel on the in vitro and in vivo regulation of P-glycoprotein. Clin. Pharmacol. Ther. 79, 11–111.
Ho, E.A., Vassileva, V., Allen, C., Piquette-Miller, M., 2005. In vitro and in vivo characterization of a novel biocompatible polymer-lipid implant system for the sustained delivery of paclitaxel. J. Control. Rel. 104, 181–191.
Kalorama Information, 2007. Drug Delivery Markets, 2nd ed., vol. II: Implantable/Injectable Delivery Systems, p. 118.
Langer, R., 1983. Implantable controlled release systems. Pharmacol. Therapeut. 21, 35–51.
Le Tien, C., Lacroix, M., Ispas-Szabo, P., Mateescu, M.A., 2003. N-acylated chitosan: hydrophobic matrices for controlled drug release. J. Control. Rel. 93, 1–13.
Lim Soo, P., Cho, J., Grant, J., Ho, E., Piquette-Miller, M., Allen, C., 2008. Drug release mechanism of paclitaxel from a chitosan-lipid implant system: effect of swelling, degradation and morphology. Eur. J. Pharm. Biopharm. 69, 149–157.
Markman, M., 1996. Regional chemotherapy: revisited. J. Cancer Res. Clin. Oncol. 122, 1–2.
Moore, G.K., Roberts, G.A.F., 1980. Determination of the degree of N-acetylation of chitosan. Int. J. Biol. Macromol. 2, 115–116.
Packhaeuser, C.B., Schnieders, J., Oster, C.G., Kissel, T., 2004. In situ forming parenteral drug delivery systems: an overview. Eur. J. Pharm. Biopharm. 58, 445–455.
Paquette, D.W., 2002. Minocycline microspheres: a complementary medical-mechanical model for the treatment of chronic periodontitis. Compend. Contin. Educ. Dent. 23, 15–21.
Rinaudo, M., Auzely, R., Vallin, C., Mullagaliev, I., 2005. Specific interactions in modified chitosan systems. Biomacromolecules 6, 2396–2407.
Roberts, G.A.F., 1992. Chitin Chemistry. Macmillan, London.
Ruel-Gariepy, E., Shive, M., Bichara, A., Berrada, M., Le Garrec, D., Chenite, A., Leroux, J.-C., 2004. A thermosensitive chitosan-based hydrogel for the local delivery of paclitaxel. Eur. J. Pharm. Biopharm. 57, 53–63.
Seong, H.S., Whang, H.S., Ko, S.W., 2000. Synthesis of a quaternary ammonium derivative of chito-oligosaccharide as antimicrobial agent for cellulosic fibers. J. Appl. Polym. Sci. 76, 2009–2015.
Sinha, V.R., Trehan, A., 2005. Biodegradable microspheres for parenteral delivery. Crit. Rev. Ther. Drug Carrier Syst. 22, 535–602.
Sonntag, N.O.V., 1953. The reactions of aliphatic acid chlorides. Chem. Rev. 52, 237–416.
Sparreboom, A., vanTellingen, O., Nooijen, W.J., Beijnen, J.H., 1996. Tissue distribution, metabolism and excretion of paclitaxel in mice. Anti-Cancer Drugs 7, 78–86.
Teomim, D., Domb, A.J., 2001. Nonlinear fatty acid terminated polyanhydrides. Biomacromolecules 2, 37–44.
Vassileva, V., Grant, J., De Souza, R., Allen, C., Piquette-Miller, M., 2007. Novel biocompatible intraperitoneal drug delivery system increases tolerability and therapeutic efficacy of paclitaxel in a human ovarian cancer xenograft model. Cancer Chemother. Pharmacol., 907–914.
Vogelhuber, W., Magni, E., Gazzaniga, A., Gopferich, A., 2003. Monolithic glyceryl trimyristate matrices for parenteral drug release applications. Eur. J. Pharm. Biopharm. 55, 133–138.
Vukelja, S.J., Anthony, S.P., Arseneau, J.C., Berman, B.S., Casey Cunningham, C., Nemunaitis, J.J., Samlowski, W.E., Fowers, K.D., 2007. Phase 1 study of escalating-dose OncoGel® (ReGel®/paclitaxel) depot injection, a controlled-release formulation of paclitaxel, for local management of superficial solid tumor lesions. Anti-Cancer Drugs 18, 283–289.
Williams, D.H., Fleming, I., 1987. Spectroscopic Methods in Organic Chemistry, 4th ed. McGraw-Hill, London, New York.
Wong, D.W.S., Gastineau, F.A., Gregorski, K.S., Tillin, S.J., Pavlath, A.E., 1992. Chitosan lipid films—microstructure and surface-energy. J. Agric. Food Chem. 40, 540–544.